Paper

Partial Discharge Characteristics in an Artificial Air-filled Void under Superimposed Sinusoidal Voltages at LN_2 Temperature

Takashi Kurihara* Student Member
Takanori Nishioka* Student Member
Junya Suehiro* Member
Masanori Hara* Member

Partial discharge (PD) characteristics within an artificial air-filled void contained in a solid insulator were experimentally investigated under superimposed sinusoidal voltages of 60 and 600 Hz at liquid nitrogen temperature (77 K) to find the effects of the waveforms of distorted sinusoidal voltages on PD characteristics at 77 K. The results show that PD inception voltage at 77 K is independent of the applied voltage waveform. The results also show that, when the 600 Hz component of the superimposed voltage is increased with its constant peak value, PD intensity seems to be independent of the voltage waveform, whereas PD pulse number increases. Since PD charge magnitude and pulse number at 77 K were remarkably different from those at 298 K, their mechanisms are discussed based on the observation results of residual charge distributions remaining on a void surface subjected to PDs under 60 Hz ac voltages at both temperatures.

Keywords: partial discharge, artificial air-filled void, liquid nitrogen temperature, superimposed sinusoidal voltage

1. Introduction

In the high temperature superconducting power equipment embedded in liquid nitrogen (LN_2), partial discharge (PD) is one of the main factors to cause degradation of its solid insulators used under cryogenic conditions. Therefore, it is necessary to clarify PD characteristics and PD degradation mechanism of solid insulators at LN_2 temperature (77 K). Furthermore, these characteristics should be investigated under not only ac voltages with commercial power frequency but also distorted ac voltages produced by operations of non-linear loads such as power electronic devices used in electric power systems [1] [2].

In this study, taking a void defect contained in a solid insulator as a PD source, fundamental PD characteristics within an artificial air-filled void were experimentally investigated under 60 Hz ac voltages at both 77 K and room temperature of 298 K. Moreover, the PD characteristics under superimposed sinusoidal voltages of 60 and 600 Hz which simulated distorted ac voltages were measured at 77 K. As a result, it is clarified that the first PD inception voltage, PD charge magnitude and pulse number at 77 K are remarkably different from those at 298 K. It is also clarified by the experiments at 77 K that PD inception voltage is almost independent of the applied voltage waveform. However, when the 600 Hz component of the superimposed voltage increases with its peak value at the PD inception level, the occurrences of PDs become synchronized with the 600 Hz component and PD pulse number increases. In order to explore the mechanisms causing the differences between PD charge magnitude and pulse number at 77 K and those at 298 K, the residual charge distributions on an inner void surface subjected to PDs were investigated at 77 and 298 K.

* Kyushu University
6-10-1, Hakozaki, Higashi-ku, Fukuoka 812-8581

2. Experimental Setup and Method

The experimental setup and the PD measurement system are the same ones as reported in the reference [3].

2.1 Applied Voltage Waveform The superimposed sinusoidal voltage v_a is defined as

$$v_a = V_l \sin(2\pi f_l t) + V_h \sin(2\pi f_h t) \cdots\cdots\cdots\cdots (1)$$

where $f_l = 60$ Hz and $f_h = 600$ Hz in this study. The summation of the peak values of the 60 Hz and the 600 Hz components, i.e. $(V_l + V_h)$, is defined as V_a. Since the difference between the real peak value of the superimposed voltage and V_a is small (less than 5%), the maximum magnitude of the applied voltages is approximated by V_a in the followings.

2.2 Test Sample Generally, the superconducting power equipment is manufactured in atmospheric air at room temperature and then operated under cryogenic conditions. Therefore, if void defects are contained in its solid insulators, the gas inside the voids is basically air, which was taken into account in our preparation for the test samples. The practical void size is presumably in the order of μm in diameter [4], but from the viewpoint of obtaining fundamental PD data, the cylindrical void with a height of 250 μm and a diameter of 5 mm was selected so that occurrences of sufficiently high PD pulses beyond the detection sensitivity (3 pC) and good reproduction of void configuration could be achieved.

In this study, two different types of electrode system are employed as a test sample. They are referred to "test samples A and B", respectively. Their schematic diagrams are shown in Fig. 1. The test sample A was used to measure fundamental PD characteristics. On the other hand, the test sample B was used for the observation of a distribution of residual charges on a solid insulator as a result of PD activities.

The artificial air-filled void in the test sample A consists of three sheets of polyethylene terephthalate (PET). The central sheet is 250 μm in thickness and has a punched hole of 5 mm in diameter at the center. The thicknesses of the other two sheets are 50 μm. These sheets are bonded tightly together with epoxy resin and placed between a high voltage sphere electrode of 5.6 mm in diameter and a grounded plane electrode of 10 mm in diameter. The electrode system is molded in epoxy resin to prevent parasitic discharges at the other locations.

The geometric arrangement of the test sample B is similar to that of the test sample A, but for simple observations of residual charge distributions, the diameters of the void and the grounded plane electrode are extended to 20 mm and the three PET sheets are not bonded with epoxy resin. Instead, in order to obtain the same gas condition within a void as that of the test sample A, the electrode system is enclosed with acrylic walls.

2.3 Observation Method of Residual Charges Remaining on a PET Sheet Residual charge distribution on a PET sheet by PDs at 298 K was easily observed by the dust figure method [5] which utilized the adhesion of charged powder (printing toner) to residual charges remaining on a solid insulator, but its use was difficult under cryogenic conditions. Therefore, these residual charges on a PET sheet were observed at 77 K by means of the frost figure method [6]. The frost figures in our case were created when a cryogenic surface of a PET sheet with residual charges touched with open atmospheric air, and water vapor in air near the charged area was attracted to the residual charges and froze. It was checked that the figures obtained by the frost figure method and ones by the toner dust figure method were almost similar.

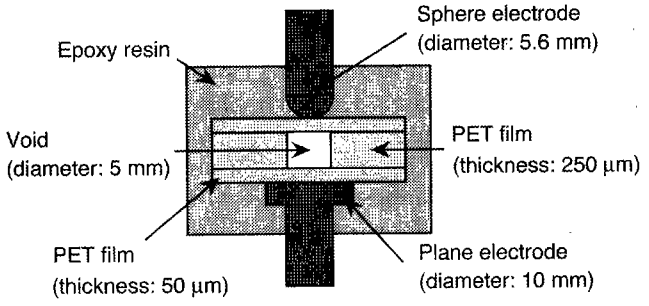

(a) Test sample A

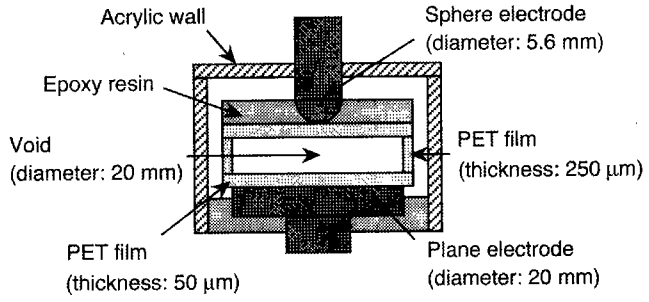

(a) Test sample B

Fig. 1. Schematic diagrams of the two types of test sample

3. Experimental Results

3.1 PD Characteristics under 60 Hz AC Voltages at Liquid Nitrogen and Room Temperatures It has been reported that PD behaviors within a void at 77 K are different from those at 298 K under 60 Hz ac voltage [7], but details of PD charge magnitude and pulse number have not been discussed. Therefore, these characteristics were investigated with the test samples A under 60 Hz ac voltages at 77 and 298 K.

3.1.1 PD inception voltage The relationships between PD inception voltages (PDIVs) and the order of the voltage applications at 77 and 298 K are shown in Fig. 2. They were measured with five test samples at each temperature. In the measurements, the peak value of the 60 Hz ac voltage was raised at the constant rate of 0.5 kV/s and it was regarded as PDIV when the first PD pulse was observed by an oscilloscope (Tektronix TDS 620A). From Fig. 2, it is found that the value of PDIV for the first voltage application is higher than those for the following voltage applications at both temperatures. Concerning the first PDIV, the value at 77 K is larger than that at 298 K. It is considered that this is because the delay time for the initial electron generation triggering the first PD ignition inside a void at 77 K is longer than that at 298 K [8]. The values of PDIV for the second or latter voltage applications are almost the same at both temperatures, and they are defined as V_i, here. With the test sample B, the similar results of PDIVs were obtained.

3.1.2 ϕ-q characteristics Figs. 3(a) and (b) are the ϕ-q characteristics measured just after the 60 Hz

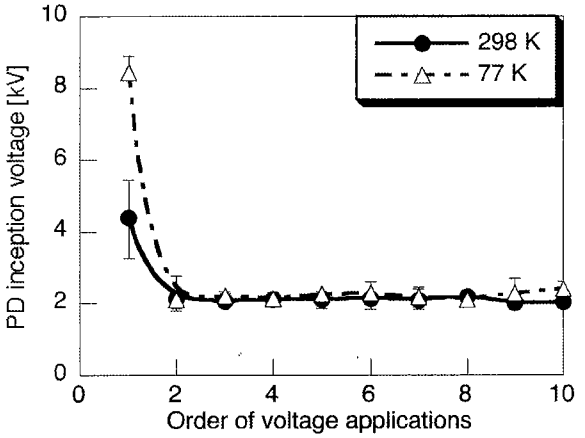

Fig. 2. PD inception voltages at 77 and 298 K as a function of the order of 60 Hz ac voltage applications

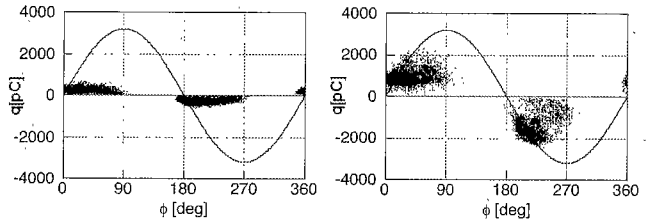

(a) 77 K (b) 298 K

Fig. 3. ϕ-q characteristics under 60 Hz ac voltage at 77 and 298 K ($V_a = 2.5$ kV)

voltage applications with $V_a = 2.5$ kV at 77 and 298 K, respectively. Here, ϕ is the phase angle of the 60 Hz ac voltage and q is the apparent PD charge magnitude. These figures depict that the values of q are distributed in the range of a few ~500 pC at 77 K while they are distributed in the wider range of 100~2500 pC at 298 K.

3.1.3 Time dependence of PD characteristics When successive PDs occur in a void, gas conditions within the void and conditions of an inner surface subjected to PDs will change [9]. Therefore, it is possible that PD characteristics such as PD charge magnitude and pulse number will vary with time. Then, the time dependence of these characteristics was measured under the 60 Hz ac voltages of $V_a = V_i$ at 77 and 298 K. The values of V_i are 2.56 kV at 77 K and 2.5 kV at 298 K.

The time dependence of the mean PD charge magnitude in 1 second q_{mean} was measured at 77 and 298 K and their results are shown in Fig. 4. From Fig. 4, it can be seen that the value of q_{mean} at 298 K is about 3~10 times larger than that at 77 K. On the other hand, the time dependence of the PD pulse number during 1 second n at both temperatures shows different features from that of q_{mean}, as reported in Fig. 5. That is, the value of n tends to be constant immediately after the voltage application and afterwards it begins to decrease to zero. Furthermore, from Fig. 5, it is found that the almost constant value of n at 77 K is about 8 times higher than that at 298 K.

From both Figs. 4 and 5, it is clear that PD pulses eventually disappear with its number decreasing, and the final PD pulse extinction comes much earlier at 298 K than at 77 K. It is believed that such time dependence of the PD characteristics is related to the changes in gas composition and surface conditions of PET sheets during the appearance of repetitive PDs, which will be described in detail in the section 4.2. Then, the results reported in Figs. 4 and 5 suggest that these changes inside the void can be more accelerated at 298 K than at 77 K.

3.2 PD Characteristics under Superimposed Sinusoidal Voltages at Liquid Nitrogen Temperature In this section, the experimental results of the PD characteristics measured with the test samples A under the superimposed sinusoidal voltages of 60 and 600 Hz at 77 K are presented.

3.2.1 Dependence of V_i on the applied voltage waveform At room temperature, it's been ensured that the value of V_i is independent of the waveform of

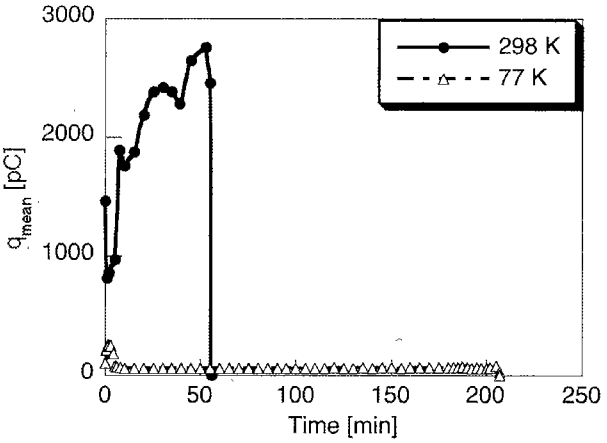

Fig. 4. Time dependence of mean PD charge magnitude in 1 second under 60 Hz ac voltage at 77 and 298 K
($V_a = V_i$; 2.56 kV at 77 K and 2.5 kV at 298 K)

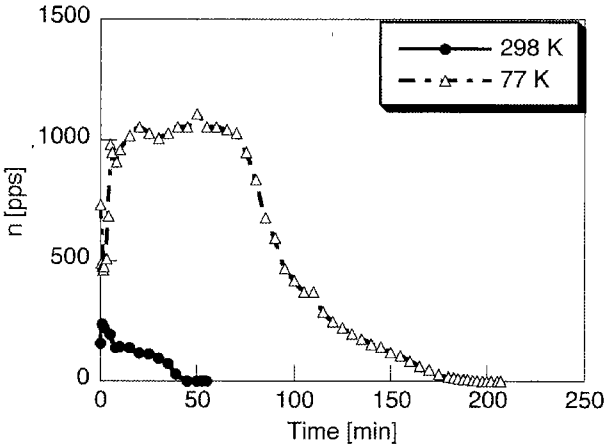

Fig. 5. Time dependence of PD pulse number during 1 second under 60 Hz ac voltage at 77 and 298 K
($V_a = V_i$; 2.56 kV at 77 K and 2.5 kV at 298 K)

the superimposed voltage [3], but its effect on V_i has not been investigated at 77 K. Then, the values of V_i were measured under the superimposed sinusoidal voltages of 60 and 600 Hz at 77 K. In the measurements, the peak value of the superimposed voltage was increased at the constant rate of 0.5 kV/s keeping the ratio V_h/V_a constant. Moreover, assuming the scattering of V_i among test samples, the same test sample was used at both 77 and 298 K. The values of V_i were measured for each voltage waveform at 77 K at first, and then the ambient temperature of the test sample was raised up to 298 K and the values of V_i were measured in the same way.

The values of V_i at 77 and 298 K are plotted as a function of V_h/V_a, i.e. the ratio of the 600 Hz component in the v_a, in Fig. 6. From the figure, it can be seen that the values of V_i at 77 K as well as 298 K are almost independent of the voltage waveform. Hence, it is believed that the effects of the applied voltage waveform on the other PD characteristics described below will have nothing to do with V_i.

3.2.2 Effect of the voltage superposition on ϕ-q characteristic Figs. 7(a)~(e) are the ϕ-q

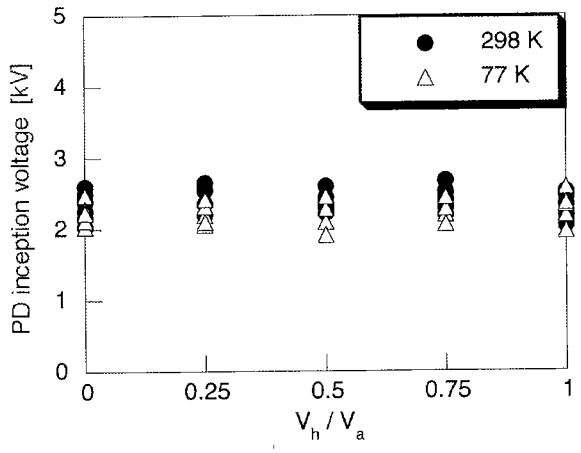

Fig. 6. V_i as a function of V_h/V_a of superimposed sinusoidal voltages of 60 and 600 Hz at 77 and 298 K

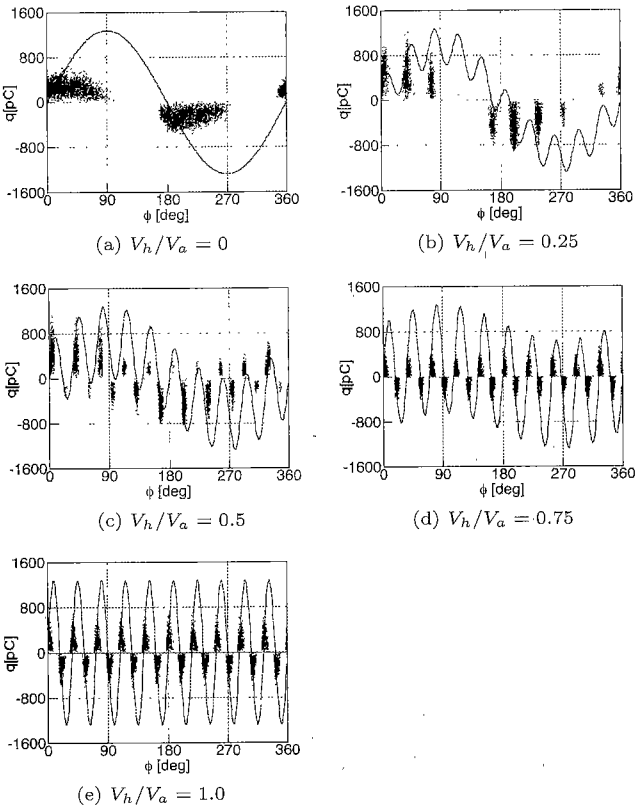

(a) $V_h/V_a = 0$ (b) $V_h/V_a = 0.25$

(c) $V_h/V_a = 0.5$ (d) $V_h/V_a = 0.75$

(e) $V_h/V_a = 1.0$

Fig. 7. ϕ-q characteristics under superimposed sinusoidal voltages of 60 and 600 Hz at 77 K ($V_a = 2.5$ kV)

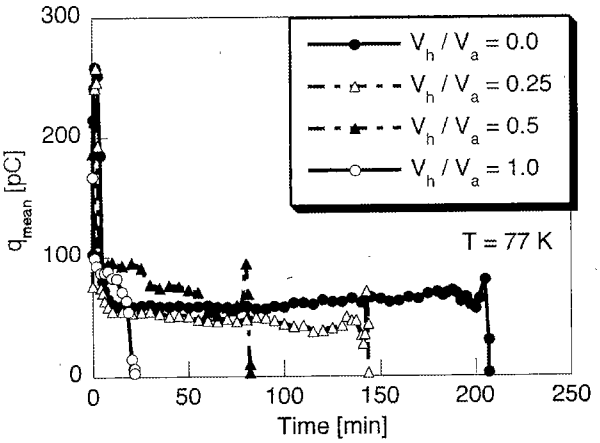

Fig. 8. Time dependence of mean PD charge magnitude in 1 second under superimposed voltages of 60 and 600 Hz at 77 K ($V_a = V_i$)

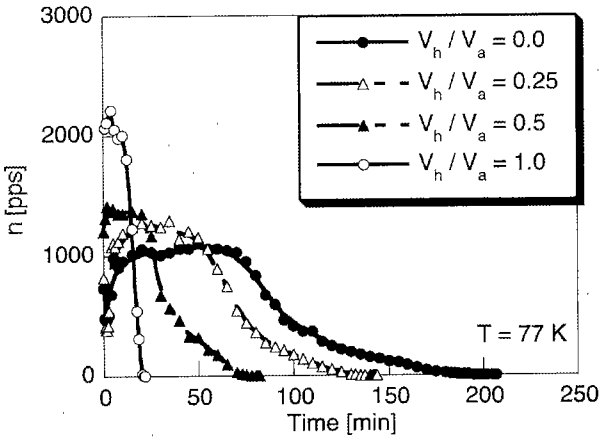

Fig. 9. Time dependence of PD pulse number during 1 second under superimposed voltages of 60 and 600 Hz at 77 K ($V_a = V_i$)

characteristics just after the applications of the voltages in the range of $V_h/V_a = 0 \sim 1.0$ with $V_a = 2.5$ kV. From these figures, the following trend can be recognized. From the ϕ-q pattern in the case of $V_h/V_a = 0.25$ (see Fig. 7(b)), the absence of PD occurrences can be seen in the regions of $\phi = 0 \sim 90°$ or $180 \sim 270°$, where PDs appear under the 60 Hz ac voltage ($V_h/V_a = 0$).

When the value of V_h/V_a is increased to 0.5, the regions of ϕ with PD occurrences can be found at every half cycles of the 600 Hz voltage component. Therefore, it can be said that the ϕ-q pattern is similar to that under the 600 Hz ac voltage ($V_h/V_a = 1.0$) in terms of the ϕ with PD occurrences, but the scattering of q at each half cycle of the 600 Hz voltage component clearly depends on the region of ϕ. For example, in Fig. 7(c), the values of q are distributed in the range of 50~1350 pC around $\phi = 40°$ where large values of q beyond 500 pC are detected in Fig. 7(a) while the values of q scatter in the narrower range of 60~300 pC around $\phi = 150°$ where no PD is observed in Fig. 7(a). From Fig. 7(c), it is also found that negative PDs appear in the region of ϕ where only positive PDs are detected in Fig. 7(a), and vice versa.

If V_h/V_a is further increased to 0.75, the ϕ-q pattern becomes similar to that under the 600 Hz ac voltage shown in Fig. 7(e).

3.2.3 Time dependence of PD characteristics

Since the PD pattern depends on the voltage waveform at 77 K as described in the previous section 3.2.2, it is predictable that the PD characteristics also depend on it. Therefore, the time dependence of the PD characteristics such as q_{mean} and n was investigated at 77 K. In the measurements, the ratio V_h/V_a was changed among A) $V_h/V_a = 0$, B) $V_h/V_a = 0.25$, C) $V_h/V_a = 0.5$ and D) $V_h/V_a = 1.0$. The value of V_a was set to V_i for each voltage waveform, and their values for the above cases

are as follows; A) $V_i = 2.56\,\mathrm{kV}$, B) $V_i = 2.46\,\mathrm{kV}$, C) $V_i = 2.84\,\mathrm{kV}$ and D) $V_i = 2.52\,\mathrm{kV}$.

The result reported in Fig. 8 represents each of the time dependence of q_{mean} for the selected values of V_h/V_a. From the figure, it is found that the values of q_{mean} for the values of V_h/V_a are different from each other just after the voltage applications, but their differences become small after the changes in q_{mean} with time become almost constant. On the other hand, the time dependence of n shown in Fig. 9 suggests that, if nearly constant values of n for the time elapse are compared among the cases A) $\sim$ D), the value of n increases with the increase in the ratio V_h/V_a. From these obtained results of q_{mean} and n, it is clear that PD charge magnitude is almost independent of the voltage waveform, but PD pulse number becomes larger as the ratio of the 600 Hz voltage component becomes higher. This means that the total PD charge magnitude during 1 second also increases with the increase in V_h/V_a.

The time elapse from the voltage application to the final PD pulse extinction becomes shorter as V_h/V_a becomes larger, as represented in Figs. 8 and 9. It is considered that this is due to the acceleration in the changes in the conditions inside the void (gas composition, void surface, etc).

4. Discussion

4.1 Mechanisms Causing the Remarkable Differences between q_{mean} and n at 77 K and those at 298 K When the void temperature T is decreased from 298 K to 77 K, PD charge magnitude remarkably decreases while PD pulse number per second greatly increases. To find the mechanisms causing these distinguished changes in the PD characteristics, residual charge distributions on a PET sheet subjected to PDs were investigated with the test samples B at 77 and 298 K.

At first, residual charge distributions just after the first PD occurrences under 60 Hz ac voltages were investigated with virgin test samples B at 77 and 298 K. Fig. 10(a) is the picture of the frost figure on a PET sheet obtained at 77 K and Fig. 10(b) is the picture of the toner dust figure on a PET sheet similarly obtained at 298 K. The values of V_a at the first PD occurrences at 77 and 298 K are 5.4 kV and 3.25 kV, respectively, and the larger value of V_a at 77 K than that at 298 K is considered to be derived from the longer delay time for the initial electron generation at 77 K than that at 298 K as explained in the section 3.1.1.

From Figs. 10(a) and (b), it is found that many traces of PD occurrences are distributed within a certain area on a PET sheet at each temperature. These charged areas by PDs were observed at the center of the void apart from the void wall at both temperatures. Therefore, it becomes clear that, in the sphere-plane electrode system employed in this study, a location of PD occurrence is not limited to the central axis of the sphere electrode but do exists around the axis. Furthermore, each area of the traces at 298 K is larger than that at 77 K. One PD trace is formed when a PD reaches a PET surface and then surface streamers slightly proceed along the PET surface from the hit site by the PD (in the direction perpendicular to the applied electric field) [10]. Thus, this observed phenomenon indicates a shorter proceeding length of the surface streamer along an inner void surface at 77 K than that at 298 K. It is believed that the remarkable decrease in the proceeding length of the surface streamer is related to the increase in the electric resistance of the PET surface as well as the decrease in the amount of the initial electron supply with the decrease in the void temperature, but these are research subjects in the future.

The charge in the distribution of residual charges from the initial one after a long exposure of a PET sheet to PDs was also investigated. The 60 Hz ac voltages of $V_a = 2.8\,\mathrm{kV}$ ($> V_i = 2.63\,\mathrm{kV}$ with the standard deviation $\sigma = 0.43\,\mathrm{kV}$) were applied to test samples B for 1 hour at 77 and 298 K, and distributions of residual charges on their PET sheets were observed. During the voltage application, q_{mean} and n were measured, and the value of q_{mean} at 298 K was about 3$\sim$8 times larger than that at 77 K while the value of n at 77 K was about 2$\sim$7 times higher than that at 298 K, and these results are similar to those obtained with the test sample A. It should be noted that steady PD pulses were observed 1 hour after the voltage application even at 298 K as well as 77 K in the case of the test sample B. Figs. 11(a) and (b) are the pictures of the frost figure on a PET sheet

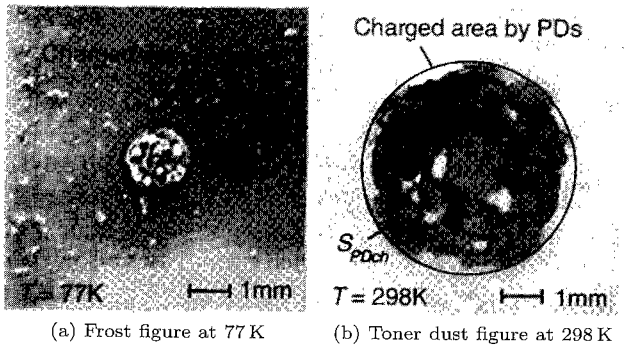

(a) Frost figure at 77 K (b) Toner dust figure at 298 K

Fig. 10. Residual charge distributions by PDs on a PET sheet just after the first applications of 60 Hz ac voltages ($V_a = 5.4\,\mathrm{kV}$ at 77 K and $V_a = 3.25\,\mathrm{kV}$ at 298 K)

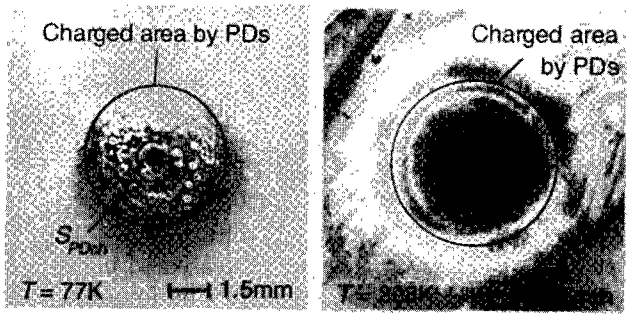

(a) Frost figure at 77 K (b) Toner dust figure at 298 K

Fig. 11. Residual charge distributions by PDs on a PET sheet 1 hour after the applications of 60 Hz ac voltages ($V_a = 2.8\,\mathrm{kV}$ at both 77 and 298 K)

1 hour after the exposure to PDs at 77 K and the toner dust figure at 298 K, respectively. From Fig. 11, it becomes clear that the total charged areas at 77 and 298 K are larger than the initial ones shown in Fig. 10, respectively, and the total charged area at 298 K is still larger than that at 77 K. It is also recognized that each area of PD traces at 77 K shown in Fig. 11(a) is still very clear and its size hardly changes from the initial ones while boundaries of PD traces at 298 K can no longer be distinguished from each other. This result confirms that the change in the composition of a PET surface subjected to PDs is much more accelerated at 298 K than at 77 K.

Based on the above observation results, the mechanisms causing the differences between PD charge magnitude and pulse number at 77 K and those at 298 K are discussed below.

On the premise that the surface charge density deployed by a single PD is uniform within the charged area denoted as S_{PDch}, the apparent PD charge magnitude q is originally expressed as the product of the effective capacitance of PET sheets charged by a single PD, C_{PETeff}, and the potential difference across the void gap at the PD ignition ΔV_g [11], and can be written by

$$q = kC_{PETeff}\Delta V_g = k\left(\frac{\varepsilon_r\varepsilon_0 S_{PDch}}{t}\right)\Delta V_g \cdots\cdots (2)$$

where k is the constant coefficient, ε_r the relative permittivity of a PET sheet, ε_0 the permittivity of vacuum, t the total thickness of two PET sheets in series with the void gap. The equation (2) states that q is directly proportional to S_{PDch}.

Then, the values of S_{PDch} at 77 K were obtained from both Fig. 10(a) and Fig. 11(a) since the change in the PET surface composition is considered to be very small even 1 hour after the voltage application at 77 K. On the other hand, the values of S_{PDch} at 298 K were obtained only from Fig. 10(b) because the boundaries of S_{PDch} in Fig. 11(b) were hard to recognize; this is thought to be caused by severe change in the PET surface composition. The results of S_{PDch} are plotted as a function of the temperature in Fig. 12. The maximum values of S_{PDch} at 77 and 298 K in Fig. 12 correspond to the traces at the center of the charged area in Fig. 11(a) and Fig. 10(b), respectively, and they are much larger than the other values at the same temperature. It is considered that this is due to an intense PD induced by the highest electric field along the central axis of the sphere electrode within a void. The other values of S_{PDch} except its maximum value correspond to the PD traces around the central one. Their average value is 0.086 mm^2 (σ = 0.052 mm^2) in the case at 77 K and 0.68 mm^2 (σ = 0.19 mm^2) in the case at 298 K.

Since the values of S_{PDch} at 77 and 298 K are very small, the uniformity of the surface charge density in S_{PDch} can be assumed. Then, from the equation (2) and the fact that the average value of S_{PDch} at 298 K is about 8 times larger than that at 77 K, it is concluded that the difference between PD charge magnitude at 77 K and that at 298 K is derived from the difference between the

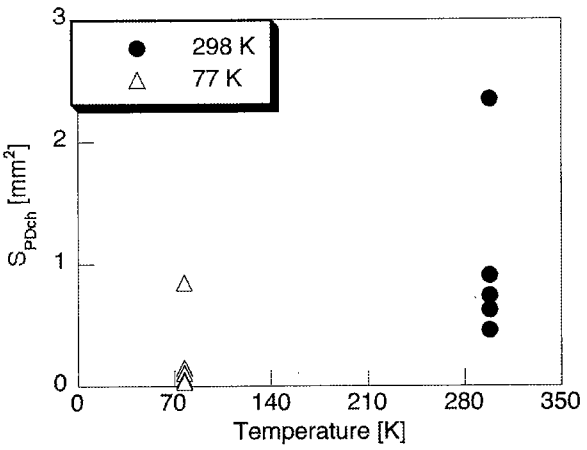

Fig. 12. Area of each PD trace at 77 and 298 K

charged area by a single PD at 77 K and that at 298 K. The latter difference is thought to be generated by the shorter proceeding length of each surface streamer just after the PD ignition at 77 K than that at 298 K.

Defining the minimum area including the total PD sites on a PET sheet as S_{PDsite}, the difference between PD pulse number at 77 K and that at 298 K can also be discussed in the following way.

As long as the direction of the electric field across a void gap doesn't change, some PDs occur within S_{PDsite}. This area of S_{PDsite} is related to the discharge volume satisfying the PD inception criterion $\int \alpha_{eff} dx = K$, where α_{eff} is the effective ionization coefficient and K is a constant value. Once a part of the void surface is charged by a PD, the net voltage across the void gap at the PD location becomes lower than the PD inception threshold. If the decay of the accumulated charges can be ignored, the succeeding PDs will not occur at the same location, especially around the voltage level of V_i, unless the direction of the electric field across the void gap is reversed. It is also considered that the neighboring charged areas dose not overlap because the tips of the surface streamers brought by the neighboring PDs have the same polarity. Therefore, the number of PDs within this time interval can be estimated by the value of S_{PDsite} divided by S_{PDch} ($= S_{PDsite}/S_{PDch}$).

The volume satisfying $\int \alpha_{eff} dx = K$ is mainly determined by the gas density inside a void ρ_{void} as well as the electric field. The value of ρ_{void} at 77 K is considered to be nearly equal to that at 298 K since the values of V_i at 77 and 298 K are almost the same (see Figs. 2 or 6). Then, it can be assumed that the value of S_{PDsite} at 77 K is equal to that at 298 K although the value of ρ_{void} can slightly vary with time as described in the next section. This assumption could be verified by the observation results shown in Fig. 10(b) and Fig. 11(a), in which the value of S_{PDsite} corresponds to the total charged area from which the total value of $S_{PDch}s$ along the border line of the total charged area is subtracted. Therefore, the value of S_{PDsite}/S_{PDch} at 77 K is much larger than that at 298 K since the value of S_{PDch} at 77 K is about an order smaller than that at 298 K, and consequently, the PD pulse number during 1 second increases with the

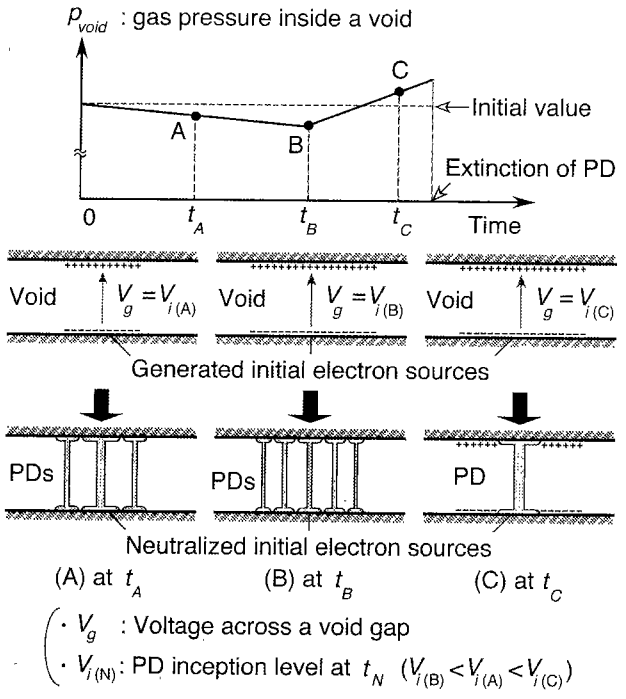

Fig. 13. Conceptual diagram of time dependence of gas pressure inside a void caused by PD activities

decrease in T.

4.2 Mechanisms Causing the Time Dependence of the PD Characteristics The clarifications of the mechanisms causing the observed time dependence of PD characteristics will need further investigations, but based on the experimental results obtained in this study, the authors give some remarks on these mechanisms with the conceptual diagram shown in Fig. 13, where the reported time dependency of the gas pressure inside a void p_{void} [12] as well as the estimated PD activities within a void at the three points in time (t_A, t_B and t_C) before the final PD pulse extinction are illustrated.

In our experiments, the measurements of the PD characteristics were performed by setting the value of V_a at V_i. This voltage V_i corresponds to PDIVs for the second or latter voltage applications, and it is much smaller than that for the first voltage application (see Fig. 2). This is because the residual charges on a PET surface become the rich initial electron sources for the successive PD occurrences. As long as repetitive PD activities continue in a void, new residual charges will be generated on a PET sheet while they will be gradually neutralized by the space charges with the opposite polarity produced by PDs as represented in Fig. 13. At the threshold level of $V_a = V_i$ for the PD appearances, it is considered that the generation and the extinction (the neutralization) of the initial electron sources will affect the PD activities.

On the other hand, as long as repetitive PDs appear inside an enclosed void, the gas pressure inside a void p_{void} keeps changing (see Fig. 13). At first, it keeps decreasing for some time ($0 \sim t_B$ in Fig. 13), and then, it begins to increase and reaches the value beyond the initial one through the change in the gas composition within a void. The decrease in p_{void} indicates the decrease in the gas density inside a void ρ_{void}, which will bring the reduction in the PD space charges and then the reduction in the neutralization of the residual charges. The decrease in p_{void} may also contribute to the enlargement of the volume inside a void satisfying $\int \alpha_{eff} dx = K$, and it could explain the slight enlargements of the possible PD occurrence areas $S_{PDsite}s$ in Figs. 11(a) and (b) from the initial ones in Figs. 10(a) and (b) at 77 and 298 K, respectively. The succeeding increase in p_{void} will bring the increase in ρ_{void}, which will contribute to the suppression of the PD occurrences.

Considering the above phenomena, the following mechanisms causing the time dependence of the PD characteristics are presumed.

At $V_a = V_i$, during the decrease in ρ_{void} or p_{void} due to the successive PD activities, the generation and the neutralization of the residual charges on a PET surface by PDs are well balanced, and the PD characteristics can maintain their steady states. However, when ρ_{void} or p_{void} begins to increase, the PD activities are gradually suppressed and finally cease. The above mechanisms will also explain the result of the earlier arrival of the PD extinction with the increase in the ratio of the 600 Hz voltage component in the superimposed sinusoidal voltage of 60 and 600 Hz at 77 K because the change in p_{void} is considered to be more accelerated with the increase in PD activities. In the actual cases, much more complex mechanisms are assumed with the contribution of the change in the composition of the PET surface subjected to PDs.

5. Conclusions

In this study, for the clarification of partial discharge (PD) characteristics under distorted ac voltages at liquid nitrogen temperature (77 K), fundamental PD characteristics within an artificial air-filled void were experimentally investigated under superimposed sinusoidal voltages of 60 and 600 Hz at 77 K. The results obtained in this study are summarized as follows.

(1) The first PD inception voltage within a virgin void is considerably larger than the second or latter ones, and the first PD inception voltage at 77 K is about twice as large as the first one at 298 K. The second or latter PD inception voltages at 77 K as well as 298 K are almost independent of the waveform of the superimposed voltage.

(2) With the decrease in the temperature within the void from 298 K to 77 K, PD charge magnitude noticeably decreases while PD pulse number remarkably increases. The former mechanism can be explained with the marked decrease in the charged area by a single PD on an inner void surface with the decrease in the temperature. The latter mechanism can also be explained by considering that the number of PDs within an identical area without any overlap of their charged areas is much larger at 77 K than the number at 298 K.

(3) When the ratio of the 600 Hz voltage component in the superimposed voltage increases with its constant peak value, PD pulse number increases although PD

charge magnitude hardly changes. This is because the PD occurrences get more synchronized with the 600 Hz voltage component as the ratio of the 600 Hz voltage component becomes larger.

(4) At 77 K, the time elapse from the voltage application to the final extinction of PD pulses becomes shorter as the ratio of the 600 Hz voltage component becomes larger. This phenomenon is considered to be caused by the acceleration in the changes in the gas conditions inside the void as well as the conditions of the inner void surface due to the increase in the PD pulse number.

(5) The above items (3) and (4) suggest that, even at 77 K, when a high frequency voltage is superimposed on an ac voltage with commercial power frequency and repetitive PD occurrences get synchronized with the high frequency voltage component, the resultant increase in PD pulse number will accelerate the degradation of the insulation systems as well as the reduction in the reliability of the high temperature superconducting power apparatus.

(Manuscript received Feb. 20, 2003,
revised June 2, 2003)

References

(1) "Recommended practices and requirements for harmonic control in electric power systems", IEEE 519 (1992).

(2) IEEE Task Force on the Effects of Harmonics on Equipment: "Effects of Harmonics on Equipment", *IEEE Trans. Power Delivery*, Vol.8, No.2, pp.672–680 (1993)

(3) T. Kurihara, S. Tsuru, K. Imasaka, J. Suehiro, and M. Hara: "PD Characteristics in an Artificial Air-Filled Void at Room Temperature under Superimposed Sinusoidal Voltages", *IEEE Trans. Dielectrics & Electrical Insulation*, Vol.8, No.2, pp.269–275 (2001)

(4) E.H. Ball, D.J.S. Skipper, W.H. Holdup, and B. Vecellio: "Development of XLPE Insulation for High Voltage Cables", Proc. CIGRE, Report No.21-01, Paris (1984)

(5) Y. Murooka and S. Koyame: "Nanosecond Surface Discharge Phenomena Study by Using Dust Figure Techniques", *J. Appl. Phys.*, Vol.44, No.4, pp.1576–1580 (1973)

(6) T. Tokunaga, H. Takazaki, and T. Isogai: "The New Observation Method of Surface Discharge Phenomena", 1973 National Convention Record IEE Japan, Vol.1, No.126, pp.169–170 (1973) (in Japanese)

(7) S. Tsuru, M. Nakamura, T. Mine, K. Sakai, J. Suehiro, and M. Hara: "PD Characteristics and Mechanisms in Artificial Air-Filled Voids at Room and Liquid Nitrogen Temperatures", *IEEE Trans. Dielectrics & Electrical Insulation*, Vol.6, No.1, pp.43–50 (1999)

(8) S. Nagata, H. Nakayama, and Y. Inuishi: "Overvoltage Dependence of Partial Discharge in Composite Dielectrics", *T. IEE Japan*, Vol.92-A, No.12, pp.545–552 (1972-12) (in Japanese)

(9) T. Tanaka: "Internal Partial Discharge and Material Degradation", *IEEE Trans. Electrical Insulation*, Vol.EI-21, No.6, pp.899–1019 (1986)

(10) L. Niemeyer: "A Generalized Approach to Partial Discharge Modeling", *IEEE Trans. Dielectrics & Electrical Insulation*, Vol.2, No.4, pp.510–528 (1995)

(11) F.H. Kreuger: Partial Discharge Detection in High-Voltage Equipment, Chapter 3, Butterworths, London (1989)

(12) Y. Kitamura and S. Hirabayashi: "Partial Discharge Characteristics and Pressure Change in a Void in Epoxy Resin", *T. IEE Japan*, Vol.105-A, No.7, pp.365–372 (1985-7) (in Japanese)

Takashi Kurihara (Student Member) was born on December 3, 1976. He entered the Master Course in the Graduate School of Information Science and Electrical Engineering (ISEE) at Kyushu University with the special promotion (the acceleration) and finished his Master Course in March 2001. He entered the Doctor Course in the same Graduate School at Kyushu University in April 2001. He has been mainly engaged in researches on partial discharge phenomena in superconducting power apparatus.

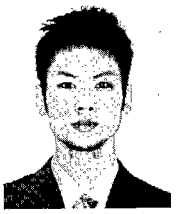

Takanori Nishioka (Student Member) was born on July 23, 1979. He entered his Master Course in the Graduate School of ISEE at Kyushu University in April 2003. He has been mainly engaged in researches on partial discharge phenomena in superconducting power apparatus.

Junya Suehiro (Member) was born on March 9, 1961. He finished his Master Course in the Graduate School of Engineering at Kyushu University in March 1985. He entered the Nippon Steel Co. in April 1985, and afterwards he became an Assistant of the Faculty of Engineering at Kyushu University in April 1988. Now, he is an Associate Professor of the Graduate School of ISEE at Kyushu University. He has been engaged in research on the electric power engineering, the applied electrostatics, the high voltage engineering and the superconductivity engineering. He has a Doctor Degree of Engineering. Dr. Suehiro is a member of the Institute of Electrostatics Japan, the Cryogenic Association of Japan and the Institute of Engineers on Electrical Discharges in Japan.

Masanori Hara (Member) was born on April 13, 1942. He finished his Doctor Course in the Graduate School of Engineering at Kyushu University in March 1972. After he served at Kyushu Institute of Technology, as a Lecturer and then as an Associate Professor, he moved to Kyushu University as an Associate Professor and was appointed as a Professor of the same university in June 1986. He has been engaged in researches on the electric power engineering, the high voltage pulsed power engineering, the superconductivity engineering and the bioengineering. He has a Doctor Degree of Engineering. Dr. Hara is a member of the IEEE Senior, the Cryogenic Association of Japan, the Institute of Electrostatics Japan and the Institute of Engineers on Electrical Discharges in Japan.